STARS

University of Central Florida
STARS

Honors Undergraduate Theses

UCF Theses and Dissertations

2022

A Novel Drug to Induce Apoptosis in Advanced Prostate Cancer Cells

Parshva A. Sanghvi
University of Central Florida

 Part of the Cancer Biology Commons
Find similar works at: https://stars.library.ucf.edu/honorstheses
University of Central Florida Libraries http://library.ucf.edu

This Open Access is brought to you for free and open access by the UCF Theses and Dissertations at STARS. It has been accepted for inclusion in Honors Undergraduate Theses by an authorized administrator of STARS. For more information, please contact STARS@ucf.edu.

Recommended Citation

Sanghvi, Parshva A., "A Novel Drug to Induce Apoptosis in Advanced Prostate Cancer Cells" (2022). *Honors Undergraduate Theses*. 1202.
https://stars.library.ucf.edu/honorstheses/1202

A NOVEL DRUG TO INDUCE APOPTOSIS IN ADVANCED PROSTATE CANCER CELLS

by

PARSHVA SANGHVI

A thesis submitted in partial fulfillment of the requirements
for the Honors in the Major Program in Biomedical Sciences
in the College of Medicine
and in the Burnett Honors College
at the University of Central Florida
Orlando, Florida

Spring Term, 2022

Thesis Chair: Robert Borgon, Ph.D.

Abstract

Prostate cancer is one of the leading causes of death for men in America with a mortality rate of approximately 1 in 41 men. In this research, we focus on enzalutamide-resistant prostate cancer cells as cell resistance to enzalutamide is a prevalent issue in treating prostate cancer. A novel compound library at different doses was tested and each compound's efficacy in inducing apoptosis in enzalutamide-resistant cells was observed. Furthermore, the mechanism by which apoptosis was induced in compounds that showed a high efficacy at lower doses was analyzed. Overall, Darapladib showed promising results in treating cells that have acquired enzalutamide resistance.

Acknowledgements

I would like to thank Dr. Robert Borgon for his mentorship and guidance during this thesis project. Thank you to Dr. Ratna Chakrabarti and Dr. Michael Strawser for serving as members on my committee. I would also like to thank Dr. Jagadananda Ghosh for allowing me to use his laboratory facilities and assisting me in the development of the project. I'd like to thank Dr. Jitender Monga for teaching me crucial assays and techniques as well as aiding me in the data collection process. Finally, I would like to thank my friends and family for their constant support in all of my endeavors.

Table of Contents

List of Tables

List of Figures

Background Information and Current Literature Surrounding Prostate Cancer

What is Prostate Cancer?

The prostate is a male reproductive gland located between the bladder and penis whose main function is to produce an alkaline fluid that both protects the sperm from the acidity of the vagina and provides sperm with better motility and nutrition. There are three major regions in the prostate, the transition, central, and peripheral zones. The transition zone comprises around 10% of the prostate region and is located "between the bladder and the upper third of the urethra" (2016). The central zone is around a quarter of the prostate's mass and is where the ejaculatory duct is found. Finally, the peripheral zone is the remaining 70% of the prostate and makes up the majority of the gland.

There are two categories of prostate tumors that take place in different regions of the prostate. Benign prostate tumors often occur in old age and take place in the transition zone. These tumors usually lead to a slight increase in the mass of the transition zone and can cause trouble in urination if the mass of the region is applying pressure to the bladder and urethra. The more cancerous tumors tend to occur in the peripheral zone and are the focus of much prostate cancer research. There are many types of prostate cancers, such as small cell carcinomas, transitional cell carcinomas, and sarcomas; however, the most prevalent form of prostate cancer are adenocarcinomas. Around 95% of all prostate malignancies tend to be adenocarcinomas (Routh, 2005). Adenocarcinoma is a type of a cancer that originates from

glandular cells. Since most of the cells in the prostate are glandular, it logically follows that most prostate cancers will be adenocarcinomas.

There are four stages of prostate cancer which are characterized by the location and spread of the malignant cells. In stages I and II, the tumor is localized and has not spread to any other region beyond the prostate. In stage III, the cancer has spread to nearby tissues and is often known as locally advanced prostate cancer. Finally, in stage IV, the cancer has spread to other parts of the body which could include vital organs such as the liver, lungs, and bones. This spread often occurs when prostate tumor cells detach and gain access to vascular pathways such as blood vessels and lymph nodes (Routh, 2005). It accomplishes this through a process known as angiogenesis where the cancer tissue is able to form new blood vessels to gain more nutrients. When the prostate cancer reaches this stage of metastasis, it is known as "advanced prostate cancer".

There are many categories of advanced prostate cancer with two major categories being castration-resistant prostate cancer and hormone-sensitive prostate cancer. Castration-resistant prostate cancer occurs when the prostate cancer cell "is growing or spreading even though testosterone levels are low from hormone therapy" (Li et al., 2016). Androgen Deprivation Therapy, a form of hormone therapy, is a treatment method often prescribed to patients with prostate cancer, through either medication or surgery, which artificially lowers the amount of testosterone in the body. This treatment is used because testosterone interacts with the prostate's androgen receptors and causes it to proliferate. Specifically, it leads to the transcription of genes that secrete peptide growth factors such as insulin-like growth factor 1 (Advanced prostate cancer, 2021). In castration-resistant prostate cancer, the cell has been able to develop

mechanisms in which it does not require the use of androgen to grow. These mechanisms include the tissue creating its own androgens, amplification of the AR proteins, and production of coactivators that do not rely on androgen binding (Hoimes & Kelly, 2010). Hormone-sensitive prostate cancer is the preliminary stage before castration-resistant prostate cancer (CRPC) has developed. In this stage, the cancer has not been exposed to any form of hormone therapy and is sensitive to treatments such as ADT and other hormone deprivation therapies. According to a metastudy done on castration-resistant prostate cancer, however, around 10-20% of prostate cancer patients develop CRPC within 5 years (ED, 2011).

Prevalence of Prostate Cancer, Mortality Rate of Prostate Cancer, and Risk Factors

Prostate cancer is the "second most frequent cancer diagnosis made in men and the fifth leading cause of death worldwide." (Rawla, 2019). It has a higher prevalence in developed countries and the chance of being diagnosed with prostate cancer increases significantly in men greater than 65 years old. The mortality rate of prostate cancer tends to be inversely related to the incident rate of prostate cancer around the globe. For example, Asian and African countries have a lower than average rate of prostate cancer incidence rates ranging around 11.5% and 26.6% respectively. However, Asian and African countries have the highest mortality rates with African countries having a mortality rate of around +124.4% and Asian countries having a mortality rate of around 116.7%. This inverse relationship can be explained by the socioeconomic conditions in Asian and African countries compared to European countries and the Americas. Developing countries often do not have the medical resources to combat prostate cancer effectively and generally detect prostate cancer in its much later stages. In comparison, the 5-year survival rate of American men who have prostate cancer tends to be 98%.

There are several risk factors that can determine the likelihood of an individual being diagnosed with prostate cancer in their lives. These risk factors consist of age, ethnicity, family history and genetics, diet, vitamins and minerals, lifestyle, and previous medical procedures. In terms of age, prostate cancer tends to affect elderly men the most. Men below the age of 50 have a 1 in 350 chance of having prostate cancer; however, this rate increases dramatically to 1 in 52 in men above 50 years old. There is a further increase after the age of 65 where the incidence of prostate cancer is around 60%. Oftentimes older men may have prostate cancer but their cause of death is a result of other conditions due to the indolent course of most prostate cancers. When looking at ethnicity, African American men have the highest rate of prostate cancer in America at a rate of 157.6. This is due to both biological and socioeconomic factors. For example, African-American men tend to have a more common chromosome 8q24 variant which has been associated with a higher rate of prostate cancer. Furthermore, African-American men tend to have less access to screening resources and thus detect prostate cancer in later stages compared to other demographics. When examining family history, approximately 20% of patients with prostate cancer have a member in their family who also have prostate cancer. This can be due to genetics but also an exposure to similar lifestyle habits. When looking at genetics, mutations in HPC genes can cause protein malfunctioning which can result in the proliferation of the cancer cells. This can be seen in a specific HPC gene known as BRCA2 which has been associated with a higher incidence of prostate cancer. A person's diet can also have an impact on their chances of having prostate cancer. Saturated animal fats promote carcinogenesis through androgens, increase reactive oxidative species, and increase tumor proliferation. Vegetables have been found to decrease the chance of prostate cancer and other cancers in general with catechins in green tea

and isoflavones in soy being especially anti-carcinogenic. Vitamins and mineral supplements can also be a factor when considering incidence rates with Vitamin D, Vitamin E, and Selenium deficiency leading to an increased rate of prostate cancer. Lifestyle choices can result in increased prostate cancer incidence rates with higher alcohol consumption, smoking, and obesity resulting in an increased rate of cancer. For example, a person consuming four alcoholic drinks a day has a relative risk of 1.21. Other lifestyle choices, such as the consumption of coffee or increased ejaculation, can have an inverse effect and may actually reduce the rate of having advanced or lethal prostate cancer. Finally, medical treatments such as diagnostic radiologic procedures and ultraviolet light exposure can cause DNA damage which could lead to mutations and eventually cancer. This is often seen in men who have undergone these medical treatments in their youth in other diseases. In summary, mortality and incident rates of prostate cancer are often inversely related due to socioeconomic and genetic differences. Furthermore, there are several risk factors ranging from age, race, diet, and more that can have a major impact on the likelihood of an individual having prostate cancer (Rawla, 2019).

Current Diagnostic Methods and Treatments of Prostate Cancer

Routine diagnosis for prostate cancer is often done after the age of 50 in males as the probability of having prostate cancer increases significantly after this age. Although 75% of prostate cancer diagnosed by standard procedures is asymptomatic (Hahn & Roberts, 1993), symptoms such as urination abnormalities and pain in the pelvic region can be an indication of prostate cancer.

Diagnosis of prostate cancer can be done through several methods, however, the most

common method tends to be a combination of the Prostate Specific Antigen (PSA) blood test and the Digital Rectal Exam (DRE). PSA is secreted by prostate tissue in the bloodstream and as the prostate tissue increases due to age the levels of PSA in a human male's bloodstream tend to increase as well. These levels can be dramatically increased, however, if the prostate has cancer as proliferation of the cancer cells can result in artificially higher levels of blood PSA. It is important to keep in mind that the rise of these PSA levels may not solely be attributed to prostate cancer. Other common conditions such as Benign Prostatic Hypertrophy (BPH) and prostatitis can also cause an artificial increase in PSA levels as the prostate tissue size increases in those conditions as well. Thus, higher PSA levels and prostate cancer have a strong association but are not always causal in relationship. There are several PSA level thresholds that physicians check for depending on the age of the patient. The recommended thresholds for men in their 40s, 50s, 60s, and 70s is "2.5, 3.5, 4.5 and 6.5 ng/mL" respectively (Osterling, Jacobsen, & Cooner, 1995). Although these PSA levels serve as benchmarks, there have been cases where a patient's levels are lower than their age's cut off and they are still diagnosed with prostate cancer. Thus, the benchmarks serve as a guide but not as definitive evidence of no cancer (Descotes, 2019). The DRE is also an important diagnostic tool as it allows the physician to examine the prostate physically for any irregularities. The physician conducts this examination by inserting a lubricated finger in the rectum and feeling the prostate gland for any lumps or enlargements. Although most patients with elevated PSA levels during screening do not have irregularities in the prostate shape, it still serves as an important tool to notice any obvious differences in the prostate (Descotes, 2019). As stated before, both the PSA Blood test and DRE

are not fool-proof measures in detecting prostate cancer but when used in conjunction can give a clearer idea if a patient has prostate cancer.

The DRE and PSA tests are often followed up with a transrectal ultrasound (TRUS) if any abnormalities are indicated in the previous two tests. The TRUS test is a biopsy test where a needle takes a random sample of the prostate for examination. Due to the random targeting of the needle, the biopsy has "a false negative rate of 15%–46% and a tumor undergrading rate of up to 38% when compared with the final Gleason score at radical prostatectomy" (Kvale et al., 2009). In order to improve the accuracy of the TRUS biopsy, a targeted MRI-TRUS fusion biopsy method is being implemented. This method targets the TRUS biopsy needle at specific regions in the prostate indicated by advanced MRI technology. This essentially reduces the rates of false negatives as it directs the needle at areas of the prostate where prostate cancer is more likely to be found. Local staging of prostate cancer along with staging of the lymph nodes is also done by this multiparametric magnetic resonance imaging (mpMRI) technology. Other technology such as a bone scan and CT scan can also be used to determine the stage of prostate cancer.

Once a patient has had a biopsy, a grade is assigned to the cancer depending on the morphology of the prostate cancer tissue. This grading system is known as the Gleason Score. The Gleason score ranges from a score of 6 to 10 with a score of 6 being classified as a low-grade cancer and a score of 8-10 being classified as a high grade cancer. This score is determined by rating the primary and secondary patterns of the cancer on a range of 3 to 5 and combining them to get a final score of 6 to 10. A score of 3 is given when the tissue looks normal while a score of 5 is given when it looks the most abnormal (Board, 2020).

Following the grading of the biopsy, the physician creates a treatment plan dependent on

several factors such as age, previous medical history, potential side effects, and the wishes of the patient. Prognosis of the treatment is dependent on these factors as well. In general there are seven types of standard treatment options that are used. These treatment options are watchful surveillance, surgery, radiation therapy, hormone therapy, chemotherapy, immunotherapy, and bisphosphonate therapy. Watchful surveillance often occurs in indolent prostate cancers that may have the potential to become malignant. In these cases, only 1 out of a 100 patients with indolent cancers die from the disease (*Localized prostate cancer: Low-risk prostate cancer: Active surveillance or treatment?*, 2020). Thus, it may not be necessary to implement active treatment measures as they may counterintuitively decrease quality of life. Surgery is often performed on patients in good health whose tumor may be removed through surgical means. Although there are many different surgery options, the most common one tends to be a radical prostatectomy. A radical prostatectomy is a procedure that removes the prostate, seminal vesicles, and surrounding tissue (Board, 2020). By removing the prostate, it significantly reduces the chance of the cancer metastasizing. However, side effects such as impotence and erectile dysfunction often follow after the completion of this procedure. Radiation therapy is another treatment option that uses high energy x-rays or other types of radiation to eliminate prostate cancer cells. There are many different types of radiation therapy from external, internal, and radiopharmaceutical. Although this mode of treatment can often be effective, it may have damaging side effects such as an increased rate of bladder and/or gastrointestinal cancer along with impotence and urinary dysfunction. Hormone therapy can also be an effective way to indirectly reduce the prostate cancer cells by reducing the amount of androgens in the body. Androgen Deprivation Therapy (ADT) is implemented in many cases of prostate cancer because testosterone and other

androgens often act to induce growth signals in prostate cells. Studies have shown that intermittent over continuous treatment of these therapies is more effective because it delays drug resistance and side effects of the therapy. By artificially reducing the amount of androgens in the body, other areas in the body that are impacted by androgens are also affected. Thus, ADT and other hormone therapy can often lead to sexual dysfunction and take a toll on the mental health of a patient. Chemotherapy is a drug-based approach where the drug is able to travel the bloodstream and destroy the cancer cells systemically. A problem with this therapy, however, is that the "mechanisms of activity of chemotherapy agents are not cancer-specific" (Beer & Bubalo, 2001). Thus, normal tissue cells around the prostate can also be susceptible to the cytotoxic effects of these drugs. Immunotherapy in prostate cancer is able to take advantage of the patient's immune system in order to fight the cancer. For example, antibodies to human CTLA-4 can help increase the function of T cells in the body and result in greater targeting of cancer cells (Madan, Gulley, & Kantoff, 2013). Another common immunotherapy is Sipuleucel-T which uses a vaccine to activate the patient's immune system. Challenges can present itself when using immunotherapy, however, including "the inability to predict treatment efficacy and patient response; the need for additional biomarkers; the development of resistance to cancer immunotherapies; the lack of clinical study designs that are optimized to determine efficacy; and high treatment costs" (Ventola, 2017). The final commonly prescribed treatment option, Bisphosphonate Therapy, mainly deals with reducing cancer spread to the bone. A side effect of Androgen Deprivation Therapy is that it often leads to an increase in bone loss. In order to combat this, bisphosphonate therapy is implemented to reduce bone fractures and reduce

metastases in the bones. Implementation of these drugs can be very effective, but can also lead to certain bone defects in other parts of the body.

Innovative treatments have also started to be used in clinical trials including cryosurgery, high-intensity-focused-ultrasound therapy, proton beam radiation therapy, and photodynamic therapy. Although these therapies show much promise, they still need to be tested more thoroughly in order to be used as more standardized treatment.

Prostate Cancer at a Molecular Level

On a molecular level, prostate cancer development and proliferation can be caused by either hereditary gene mutations or sporadic gene mutations. Although most cases fall in the sporadic prostate cancer category, around 42% can also be accounted for by heritable factors (Lichtenstein et al., 2000). According to studies done on familiar inheritance of prostate cancer, genes associated with prostate cancer can be transferred through all three modes of inheritance (autosomal dominant, recessive, and X-linked) (Lichtenstein et al., 2000). The two main autosomal genes to be identified in prostate cancer inheritance are HPC1/RNASEL and PCAP. RNASEL is a ribonuclease involved in the degradation of cellular and viral mRNA along with inducing apoptosis in viral infections. Although not confirmed by all studies, many have pointed that mutations in this ribonuclease may result in inhibition of anti-proliferative mechanisms of the ribonuclease allowing further growth of the prostate cancer tumor. Another gene that may play a crucial role in hereditary prostate cancer is CHEK2. CHEK2 regulates p53 in the DNA damage signaling pathway (Mazaris & Tsiotras, 2013). Thus, mutations in this gene may result in malfunctioning of tumor suppressing mechanisms which could lead to increased tumor proliferation in prostate cancer cells.

When looking at sporadic prostate cancer, the two main gene types that develop mutations are tumor suppressor genes and proto-oncogenes. The most commonly mutated tumor suppressor gene is the p53 gene. The p53 gene has a relatively low mutation rate in primary prostate cancer, 10-20%, but tends to be highly mutated in advanced prostate cancer, approximately 42% of the time. Proper functioning of the p53 is crucial as it acts as a checkpoint before a cell goes to the S phase in mitosis as well as inducing apoptosis in cells that have damaged DNA. Another important tumor suppressor gene is CDKN1B which codes for p27 – a cyclin dependent kinase inhibitor that often has reduced cellular levels during advanced stages of prostate cancer. Mutations in the CDKN1B gene resulting in a non-functioning p27 may also lead to loss of PTEN function, another tumor suppressor gene that is important in cell regulation. PTEN acts as a tumor suppressor by "inhibiting the phosphatidylinositol 3-kinase-protein kinase B (PKB-Akt) signaling pathway which is essential for cell cycle progression and cell survival" (Sun et al., 1999). The main proto-oncogene associated with prostate cancer is c-MYC. c-MYC is a transcription factor that belongs to a family of helix-loop-helix-leucine zipper proteins (Garcia-Gutierrez, Delgado, & Leon, 2019). c-MYC promotes cell proliferation by inducing "positive cell-cycle regulators such as cyclins, CDK's, and E2F transcription factors" (Garcia-Gutierrez, Delgado, & Leon, 2019). It also inhibits many of the common cell-cycle inhibitors such as p15, p21, and p27. Although c-MYC in normal concentrations is not detrimental to the cell, over-expression of this protein can result in greater tumor growth as seen in about 30% of advanced prostate cancer cases (Mazaris & Tsiotras, 2013). Another common proto-oncogene in prostate cancer cells is Bcl-2. Bcl-2 is not commonly expressed in normal prostate cells; however, it is commonly expressed in advanced prostate cancer cells. Studies have shown that

Bcl-2 overexpression may be a result of androgen-independent prostate cancer as androgens tend to down-regulate the expression of Bcl-2. Bcl-2 overexpression often leads to the safeguard of prostate cancer cells from apoptosis.

Although mutations in both proto-oncogenes and tumor suppressor genes lead to development of prostate cancer cells, intracellular receptors also play a major role in the development of prostate cancer. The main intracellular receptor involved in prostate cancer is the androgen receptor. DHT, produced by the conversion of testosterone via 5α-reductase, is able to attach to the androgen receptor with great affinity once it enters prostate cells (Lonergan & Tindall, 2011). Once bound to the AR, the AR is able to enter the nucleus and bind to the DNA acting as a transcription factor. This propagates the further proliferation of the prostate cancer cells. Although hormone deprivation therapy is often used to combat this issue, it is generally a temporary solution. This is because the cell is able to find other mechanisms by which the Androgen Receptor can still be activated or ways by which the androgen receptor pathway can be bypassed to produce the same outcomes. For example, when studying metastatic prostate cancer cells point mutations in the AR gene from CAA to CGA or GCC to ACC were detected. These mutations prevented the drug analog to bind to the active site. Advanced prostate cancer cells have also been found to express higher levels of AR transcripts allowing for there to be a higher concentration of Androgen receptors within the cell (Mazaris & Tsiotras, 2013). This gives the prostate cancer cell the ability to compensate for the artificially lowered levels of androgens through Androgen Deprivation Therapy (ADT).

Common Apoptosis Pathways and Mechanisms

Apoptosis is a process by which a cell undergoes programmed death. Apoptosis is a

normal process and tends to occur during the development of the cell along with acting as a mechanism to regulate cell populations in tissue (Elmore, 2007). In this project it is important to understand the mechanism by which apoptosis occurs as a majority of the compounds involved in limiting the proliferation of prostate cancer cells induce apoptosis in the cell. The process of apoptosis is often compared to necrosis as both processes lead to the death of a cell. However, there are several key factors that differentiate the process of apoptosis and necrosis. Apoptosis is a deliberate process and involves an energy-dependent mechanism. In contrast, necrosis is a passive process usually caused by some cytotoxicity in the environment. It is not an energy dependent mechanism and often affects contiguous cells. Apoptosis usually occurs in a single cell and results in the shrinking of the cell with the cytoplasm retained in apoptotic bodies (Elmore, 2007), while necrosis causes cell swelling and the release of cytoplasm in the environment. Although apoptosis is generally considered an irreversible process, scientists have identified certain conditions in which it can be reversed. For example, mutations in engulfment genes sometimes allow for the survival and differentiation of cells that were destined for apoptosis (Reddien, Cameron, & Horvitz, 2001). Generally, weak apoptotic signals and mutations/removal of macrophages and other engulfment mechanisms may allow the cell to survive even if caspase has been activated.

When examining the mechanism of apoptosis there are three main pathways by which a cell conducts apoptosis. These pathways are the extrinsic pathway, intrinsic pathway, and perforin/granzyme pathway. All of these pathways utilize caspase proteins which are typically in their inactive form and when activated can initiate the activity of other procaspases, leading to a protease cascade (Elmore, 2007). The rapid activation of these caspase dependent transduction

signals allows the cell to amplify apoptosis and lead to rapid cell death. The extrinsic pathway is also commonly referred to as the "death receptor pathway", while the intrinsic pathway is referred to as the "mitochondrial pathway". Although these pathways may seem independent, recent studies have shown that certain steps may be interrelated (Igney & Krammer, 2002). All three pathways also converge at a single point, known as caspase-3, and continue uniformly down a path known as the "execution pathway". The execution pathway relies on a transmembrane death receptor that is part of the Tumor Necrosis Factor (TNF) super family of receptors. There are many death ligands that bind to this receptor with some examples being FasL/FasR, TNF-*a*/TNFR1, and Apo3L/Dr3. The binding of the death ligand induces a clustering of receptors which recruit several different adaptor molecules. These adaptor molecules help facilitate the formation of a death signaling complex more commonly known as DISC. Once DISC is formed, it activates caspase-8 which activates caspase-3. At this point, the cell enters into the execution pathway. The intrinsic pathway is activated by receptor-independent stimuli and is divided into negative and positive stimuli. Positive stimuli are stimuli that lead to the activation of apoptotic pathways. These stimuli include radiation, toxins, hypoxia, etc. Negative stimuli, on the other hand, are stimuli that do not activate apoptosis directly but rather inhibit apoptotic suppression mechanisms. Both stimuli lead to the opening of the mitochondrial permeability transition pore (MPT), which leads to the increased permeability of the inner mitochondrial membrane. This increased permeability has two effects: the dispersion of the proton gradient and the release of pro-apoptotic proteins. The dispersion of the proton gradient significantly reduces the amount of ATP generated by the cell and results in energy deficiency. The release of pro-apoptotic proteins results in the formation of a protein called

apoptosome, which leads to caspase 9 activation. Caspase 9 is able to activate caspase-3 that then leads the cell into the execution pathway. The perforin/granzyme pathway is activated by cytotoxic T (CD8+ cells) in response to antigen markers on the cell surface indicating signs of infection. In response to these antigens, the cytotoxic T cell creates a transmembrane perforin molecule, which releases granules containing granzyme B and granzyme A. Granzyme B has the ability to both directly activate caspase-3 and indirectly activate caspase-3 through caspase-10 activation. As mentioned before, once caspase-3 is activated the cell activates the execution pathway. Granzyme B can utilize the mitochondrial/intrinsic pathway to accomplish apoptosis. Granzyme A is able to induce apoptosis through caspase-independent mechanisms. It can accomplish this by cleaving the SET complex that has a role in DNA repair. By cleaving this SET complex, the DNA is more prone to cleavage by DNAases, which eventually results in the degradation of DNA. As mentioned before, all three pathways converge at the execution pathway. Thus, it is important to understand how the execution pathway is utilized to induce apoptosis in the cell. The execution pathway is triggered by the activation of caspase-3 and once caspase-3 is activated, the two main proteins that it activates are endonucleases and proteases. In terms of endonucleases, the main endonuclease activated is CAD which is cleaved from its inactive form, ICAD, by caspase-3. CAD is responsible for degrading chromosomal DNA and condensing chromatin. In terms of proteases, caspase-3, caspase-6, and caspase-7 work in conjunction to cleave several cytoplasmic and nuclear proteins such as alpha fodrin and NuMA. The final phase of apoptosis is phagocytic uptake of the cell. This phase is characterized by the presence of phosphatidylserine on the outer leaflet of the cell membrane which signals for phagocytic recognition, uptake, and disposal in a noninflammatory fashion (Fadok, Cathelineau,

Henson, Bratton, & Daleke, 2012). Identifying which apoptotic pathway is used by a novel compound will help further our understanding of the mechanism by which proliferation of the prostate cancer cells is inhibited.

Specific Aims of the Project

1. Test a library of novel compounds on advanced prostate cancer cells and assess the rate at which the cells are proliferating in comparison to untreated cells.
2. Identify a compound from the library that has the potential to inhibit proliferation of advanced prostate cancer cells. Furthermore, identify a compound that has cytotoxic effects and has the ability to induce apoptosis specific to advanced prostate cancer cells.
3. Once a novel compound has been identified with the ability of inducing apoptosis in advanced prostate cancer cells, understand the apoptotic mechanism by which it is able to cause cell death in these cells.

Methods

Drug Culturing Assay and Prostate Cancer Cell Line

To conduct the drug screening and viability assay I selected the Lymph Node Carcinoma of the Prostate Enzalutamide Resistant (LNCaP-ENR) cell line. The LNCaP cells were prostate cancer cells that have been desensitized to enzalutamide drugs. These types of cells are normally present in stage I-II of prostate cancer (Ravenna et al., 2014).

In order to maintain these cell lines, several reagents were used. Initially, the cells (~300,0000) were plated in a 60 mm diameter plate (Falcon) with RPMI 1640 (Thermo Fisher Scientific) media and 10% Fetal Bovine Serum (FBS). The RPMI 1640 media contains important nutrients for the cell to survive including Biotin, Vitamin B_{12}, and PABA, while the 10% FBS includes growth factors and antibodies to aid in cell growth and immunity. The cells were incubated at 37°C for 48 hours in a CO_2 incubator. Once the plates have reached 70% confluency, the cells were divided into half in order to prevent stationary/death phase. The confluency of the cell plate was verified by observing the tissue plate under a compound microscope. There were several steps taken to reduce the cell population in half. First, the old media was discarded and Dulbecco's Phosphate-Buffered Saline (dPBS) was added to remove any cellular junk from the plate. Once the dPBS had taken up all of the cellular junk it was also discarded in the same manner as the old media. In order to lift the cells off of the plate, trypsin was added and the cells were incubated with the trypsin mixture for a couple of minutes. It is important not to prolong this step as long term cellular exposure to trypsin can actually be damaging to the cell line. After a couple of minutes, the trypsin was neutralized with 2-3 times the amount of RPMI 1640 and 10% FBS. The cellular mixture was then homogenized through

micropipetting and half of the mixture was transferred to a new plate. Thus, the new plate had 50% of the cells from the old plate and the old plate was discarded. The new plate also received additional RPMI 1640 media with 10% FBS in order to ensure proper growth of the cells. The final plate was incubated at 37℃ and the reduction process was repeated after another 48 hours. The proper maintenance of these cells was crucial in receiving accurate data when these cells were treated with varying novel compounds in the drug screening and viability assay (Ghosh, 2004).

Drug Screening Assay

The drug screening and viability assays allow us to test several novel compounds at different dosages and assess their ability to induce apoptosis in the cancer cell lines. In order to run this assay, approximately 2,500 cells were seeded per well in a 96 well plate. Each well also consisted of RPMI and 10% FBS to ensure the survival of the cells in the well. The total volume in each well was standardized to a 100 µL. The 96 well plate was then incubated for 72 hours at 37℃ in a CO_2 incubator. Along with the cells being based in the RPMI media and 10% FBS, the cells also received a varying dosage of different novel compounds. Furthermore, there were a couple of cell wells that did not receive any dosage of the drug to serve as the control. The dosage of each compound increased in constant increments depending on the strength of the compound. Once 72 hours had passed, the viability of the cells was checked through an MTS/PES One Solution Cell Titer Assay (Promega Corp, Madison, WI).

MTS/PES One Solution Cell Titer Assay and Cell Viability

The MTS/PES One Solution Cell Titer Assay was used to determine the number of cells

that were still viable in a well after 72 hours of administering a certain dosage of a novel compound in the well. This assay primarily works by detecting the amount of ATP in a well and correlating the amount of ATP to the presence of metabolically active cells. In the MTS/PES One Solution Cell Titer Assay, the main compound that reacts with ATP is Luciferin. The reaction is catalyzed by magnesium and results in fluorescence of the compound once the reaction is completed. The level of fluorescence of each individual well was detected by a plate reader and absorption values were read through a connected monitor. These absorbance values were then used to determine the amount of ATP in the solution which was correlated to the amount of viable cells in the solution. Promega provides a standard curve correlating absorbance values and the number of cells in a solution as long as the cell media volume of each well in the 96 well plate is at a 100 µL. When looking at the MTS/PES One Solution Cell Titer Assay protocol, the first step required was the thawing of the Cell Titer Assay reagent from -70℃ to room temperature. It was important to have this temperature change take place gradually as a sudden change in temperature could have lead to the breaking of the tube. Furthermore, it is recommended not to have the reagents exceed a temperature of 25℃ as it can cause the reagents to denature. Once the Cell Titer Assay reagent had been properly thawed, 20 µL was added to each of the 100 µL cell media volumes in the 96 well plate. It was crucial to keep the reagent in a dark environment prior to addition as it prevented the fluorescence process from beginning early. Once the reagent had been added, the 96 well plate was shaken for two minutes in order to properly homogenize the mixture and allow the cells to lyse. After the two minutes were over, the plate was incubated at 37℃ for ninety minutes in order to allow the reaction between the luciferase and ATP to properly take place. By performing this assay, analysis of which

compounds were more effective in inducing apoptosis in the cancer cell lines becomes much simpler (*Cell-Titer Glo 2.0 Assay,* 2018).

Experimental Design

Collecting data for each novel compound took place over a week. Each week, cells were seeded in the 96-well plate using the existing cell line, novel compounds were added in a dose dependent manner, and the MTS assay was conducted. The sections below go into detail regarding each of these phases.

Seeding 96-Well Plate

Before seeding the 96-well plate, the 60 mm cell plate containing the cell line was first observed under a microscope for confluency and contamination. Once the cells were ensured to be healthy and in proper confluency, they were trypsinized in order to detach from the 60 mm cell plate. RPMI media was then added to the mixture and the cells were aspirated thoroughly to maintain homogeneity. Approximately 500 µL was taken from the mixture and placed in a ViCell Cell Counter to determine the total cell count of the plate. The ViCell Cell Counter used Trypan Blue Dye to stain the cells in the 500 µL sample and differentiate between viable and non-viable cells.

Once the total cell count of the 60 mm cell plate was obtained, a dilution mixture was created consisting of cells and media to achieve a cell concentration of 2,500 cells per 100 µL. In order to avoid contamination, only the internal wells were seeded with cells. Thus, only 60 wells out of the 96 wells were seeded. Each well consisted of 2,500 cells and 100 µL of total volume. The dilution mixture was created with a total volume of 6.5 mL instead of 6 mL to account for any margin of error in the pipettes. All the wells were pipetted in a column-by-column manner and with approximately the same angle to maintain a controlled environment. Once all of the 60 wells were seeded, the 96-well plate was kept at 37°C in a CO_2 incubator for 24 hours.

Addition of Novel Compounds

Prior to the addition of the novel compounds, the 96-well plate was observed under a microscope to ensure that each well had the same number of cells and that the cells were attached in approximately the same location. Initially, many wells were removed as they did not contain the same number of cells resulting in fewer novel compounds being tested. As the project continued, however, the consistency in pipetting the wells improved and more compounds were tested at a time. Once any erroneous wells were crossed out, the remaining wells were labeled with both the drug that was going to be added as well as the concentration.

Initially, all of the novel compounds came in a 50 mM stock concentration. Since most of the dosages fell between 2 μM to 30 μM, the compounds had to be diluted using 10% DMSO. Once the proper dilutions had been created, each dose was added in a triplicate in order to minimize the margin of error. In addition, three wells were kept as controls with no novel compounds added and three wells solely consisted of media to act as a blank. The novel compounds were pipetted into the wells in an identical manner and the control wells were located in close proximity to the experimental wells to replicate similar conditions. Once all of the novel compounds were added, the 96-well plate was kept at 37℃ in a CO_2 incubator for 72 hours. In the beginning of the project, only two novel compounds at different dosage concentrations were tested at a time. As time went on, however, around four novel compounds were tested at different dosage concentrations at a time. This allowed for a significant increase in the total number of novel compounds that were able to be screened by the end of the project.

Conducting MTS Assay

To initiate the MTS assay, the MTS reagent is thawed gradually from a temperature of -70 ℃ to room temperature using a water bath. During this thawing process, the reagent is kept in a dark environment to prevent the reagent from reacting with light prior to addition. Once the reagent has been thawed, 20 μL of the reagent is added to each of the internal wells in the 96-well plate. The reagent is pipetted in an identical manner to reduce the margin of error. After adding the reagent, it is lightly shaken for two minutes allowing the mixture to homogenize. Then, the 96-well plate is kept at 37℃ in a CO_2 incubator for 90 minutes as the luciferase and ATP need adequate time to react. Subsequently, the 96-well plate is then placed in a "blank" machine where the absorbance value for each well is recorded. The MTS reagent becomes a darker color with greater cellular activity. Thus, an effective novel compound would exhibit a lighter color as the dosage of that compound increases in comparison to the control well.

Results

Apalutamide

Table 1: LNCaP-ENR Percent Cell Viability at Various Apalutamide Concentrations

Percent Cell Viability		
10 µM	**20 µM**	**30 µM**
74.82394366	102.8169014	107.3943662
73.5915493	100.8802817	100.528169
88.55633803	95.42253521	111.971831

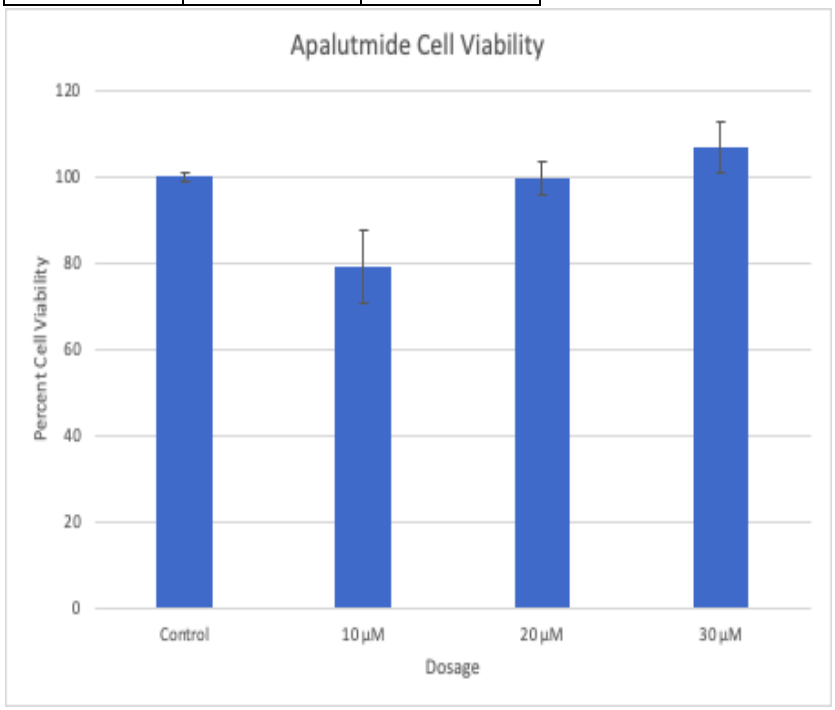

Figure 1: Bar Graph Indicating Mean Percent Cell Viability for LNCAP-ENR cells at different concentrations of Apalutamide

NVP-TAE 226

Table 2: LNCaP-ENR Percent Cell Viability at Various NVP-TAE 226

Percent Cell Viability				
0.5 µM	**1 µM**	**2 µM**	**4 µM**	**8 µM**
89.57415565	115.712188	102.8879099	85.26676456	72.7361723
79.78463045	109.8384728	95.05628977	74.30249633	74.79197259
88.88888889	86.93098385	87.71414586	76.84777288	70.87616251

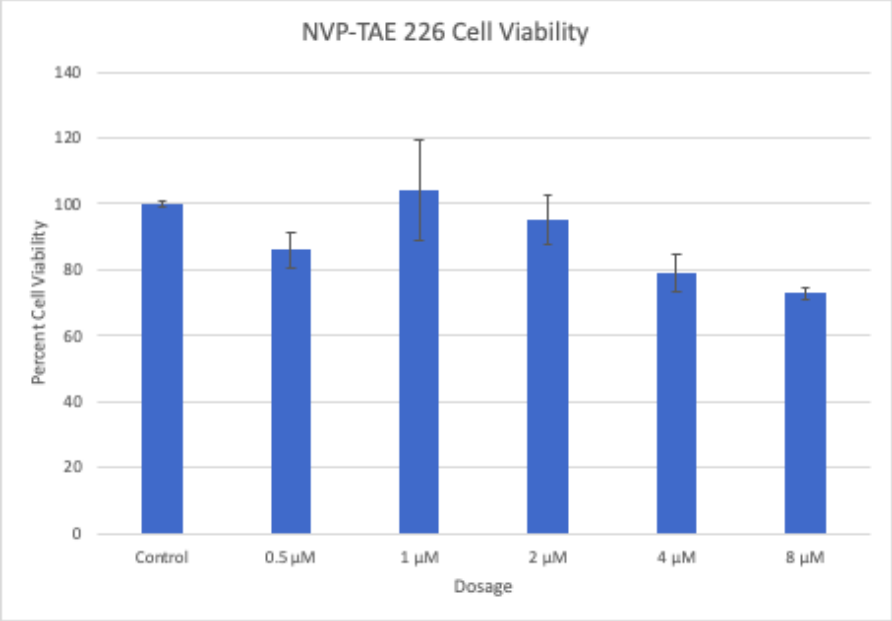

Figure 2: Bar Graph Indicating Mean Percent Cell Viability for LNCAP-ENR cells at different concentrations of NVP-TAE 226

LRRK2-IN-1

Table 3: LNCaP-ENR Percent Cell Viability at Various LRRK2-IN-1 Concentrations

Percent Cell Viability				
0.5 µM	**1 µM**	**2 µM**	**4 µM**	**8 µM**
124.1311796	103.3773862	92.70680372	59.71610377	43.66128243
121.7816936	94.66470876	84.28781204	55.80029369	40.92021537
122.0753793	92.51101322	75.28144885	54.23396965	38.86441508

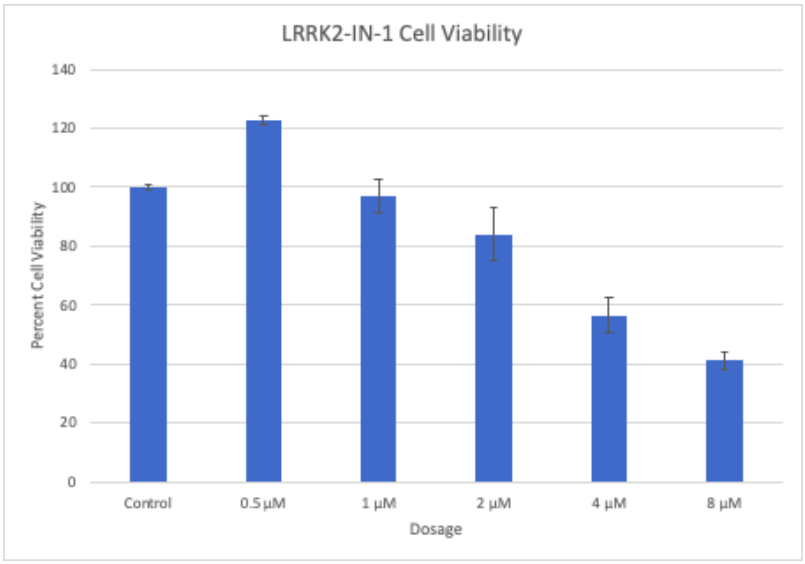

Figure 3: Bar Graph Indicating Mean Percent Cell Viability for LNCAP-ENR cells at different concentrations of LRRK2-IN-1

AZD-9291

Table 4: LNCaP-ENR Percent Cell Viability at Various AZD-9291 Concentrations

Percent Cell Viability				
1 µM	**2 µM**	**4 µM**	**8 µM**	**12 µM**
96.37023593	78.0399274	49.00181488	3.992740472	1.633393829
98.00362976	77.31397459	33.75680581	4.355716878	2.359346642
95.09981851	66.4246824	35.93466425	4.718693285	2.359346642

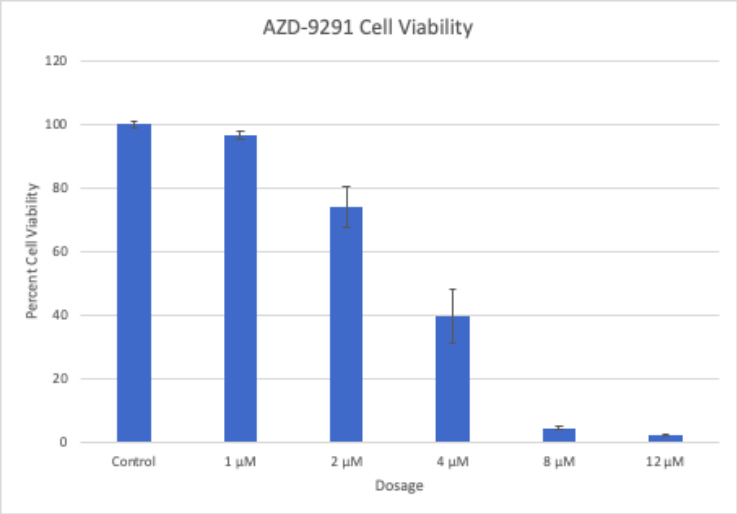

Figure 4: Bar Graph Indicating Mean Percent Cell Viability for LNCAP-ENR cells at different concentrations of AZD-9291

XMD8-92

Table 5: LNCaP-ENR Percent Cell Viability at Various XMD8-92 Concentrations

Percent Cell Viability				
1 µM	**2 µM**	**4 µM**	**8 µM**	**12 µM**
102.1778584	80.03629764	45.91651543	27.5862069	14.15607985
106.7150635	107.2595281	42.46823956	23.04900181	17.78584392
110.3448276	79.67332123	54.08348457	23.95644283	15.60798548

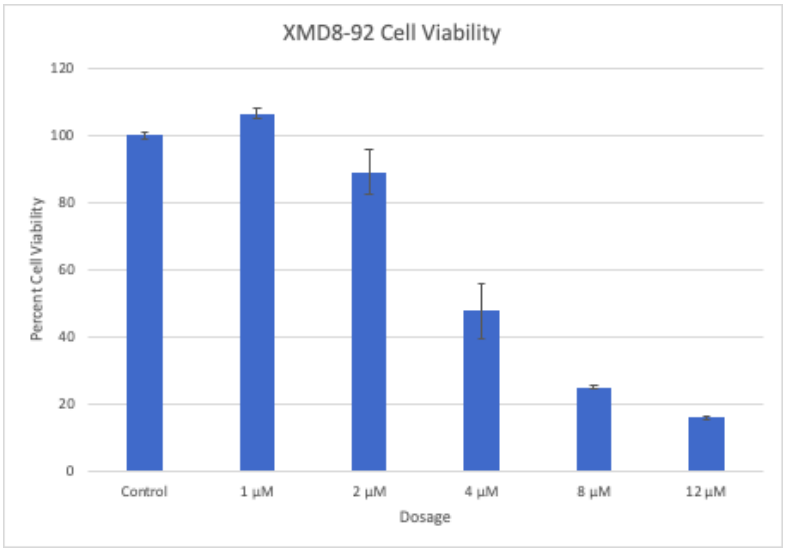

Figure 5: Bar Graph Indicating Mean Percent Cell Viability for LNCAP-ENR cells at different concentrations of XMD8-92

Ibrutinib

Table 6: LNCaP-ENR Percent Cell Viability at Various Ibrutinib Concentrations

Percent Cell Viability				
1 µM	**2 µM**	**4 µM**	**8 µM**	**12 µM**
113.430127	105.2631579	109.9818512	114.3375681	84.75499093
110.3448276	112.522686	110.8892922	100.1814882	88.02177858
100.5444646	99.8185118	104.7186933	103.6297641	74.77313975

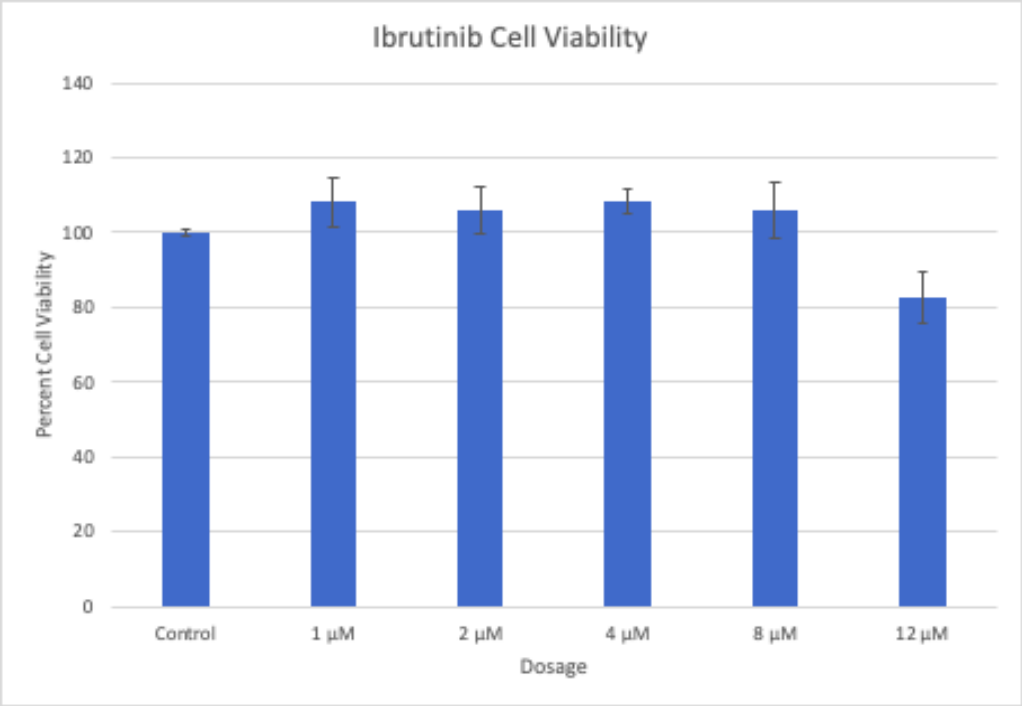

Figure 6: Bar Graph Indicating Mean Percent Cell Viability for LNCAP-ENR cells at different concentrations of Ibrutinib

CEP-37440

Table 7: LNCaP-ENR Percent Cell Viability at Various CEP-37440 Concentrations

Percent Cell Viability				
1 µM	**2 µM**	**4 µM**	**8 µM**	**12 µM**
100	113.5542169	91.26506024	40.96385542	196.3855422
125.6024096	62.95180723	412.6506024	51.80722892	-1.204819277
126.5060241	77.10843373	80.72289157	50.90361446	-3.915662651

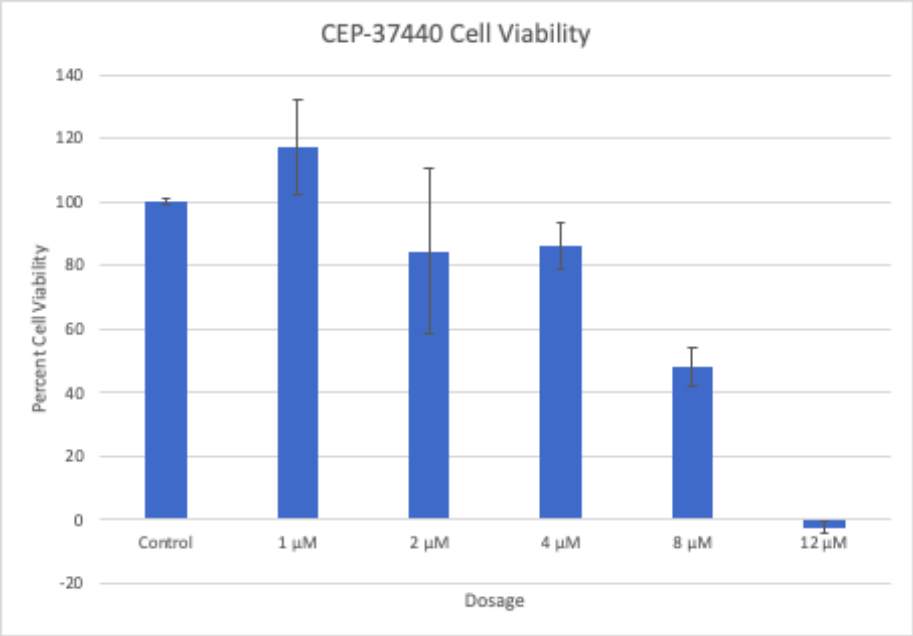

Figure 7: Bar Graph Indicating Mean Percent Cell Viability for LNCAP-ENR cells at different concentrations of CEP-37440

Abiraterone

Table 8: LNCaP-ENR Percent Cell Viability at Various Abiraterone Concentrations

Percent Cell Viability		
10 µM	**20 µM**	**30 µM**
100.695825	95.92445328	101.6898608
118.2902584	113.916501	130.5168986
139.860835	111.4314115	121.1729622

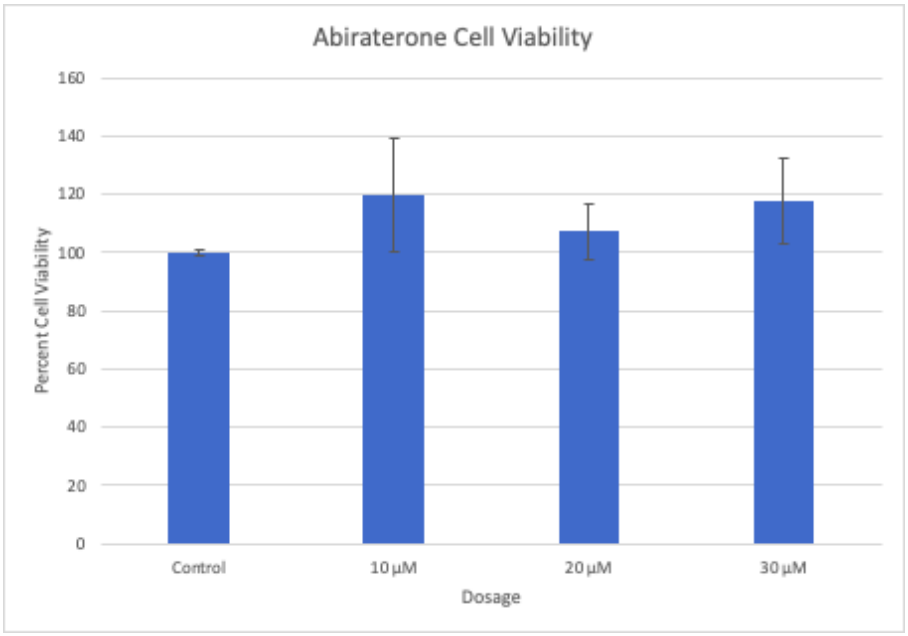

Figure 8: Bar Graph Indicating Mean Percent Cell Viability for LNCAP-ENR cells at different concentrations of Abiraterone

Darolutamide

Table 9: LNCaP-ENR Percent Cell Viability at Various Darolutamide Concentrations

Percent Cell Viability		
15 µM	**20 µM**	**30 µM**
151.2922465	97.41550696	92.64413519
116.2027833	107.4552684	108.9463221
157.8528827	102.8827038	102.8827038

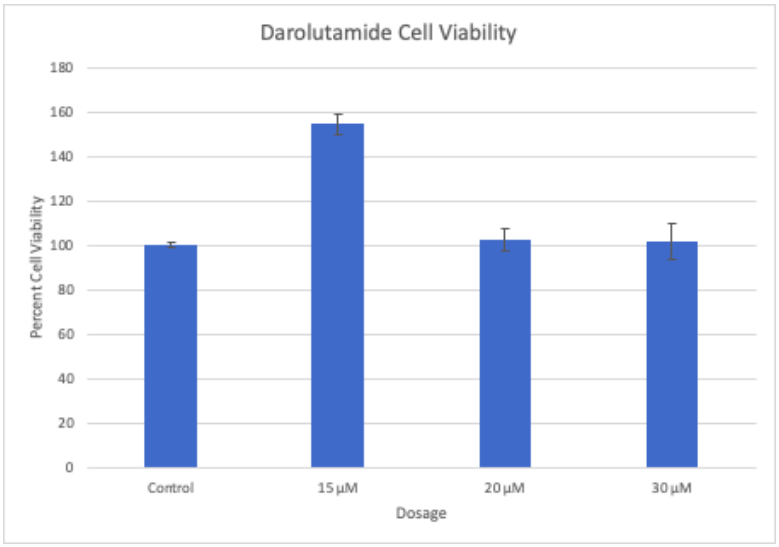

Figure 9: Bar Graph Indicating Mean Percent Cell Viability for LNCAP-ENR cells at different concentrations of Darolutamide

Daclatasvir Impurity B

Table 10: LNCaP-ENR Percent Cell Viability at Various Daclatasvir Concentrations

Percent Cell Viability		
6 µM	**8 µM**	**12 µM**
103.4791252	104.9701789	92.44532803
104.0755467	71.66998012	87.67395626
99.70178926	69.28429423	96.42147117

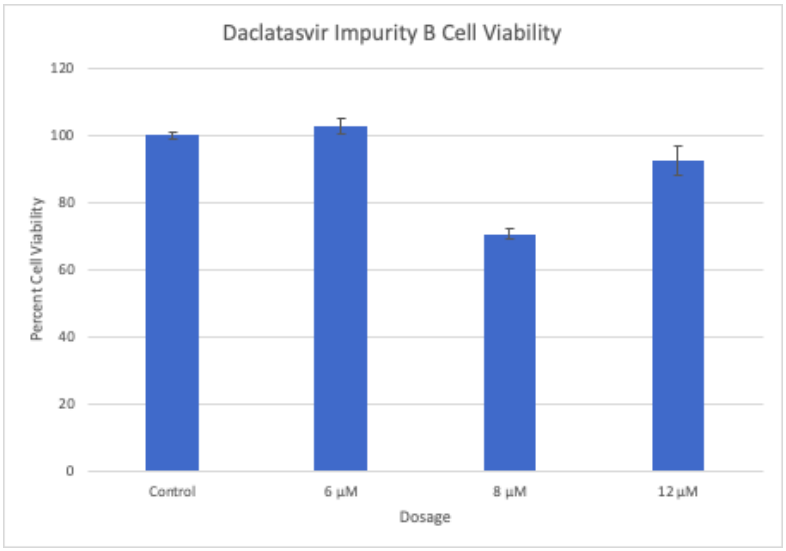

Figure 10: Bar Graph Indicating Mean Percent Cell Viability for LNCAP-ENR cells at different concentrations of Daclatasvir Impurity B

Daclatasvir Impurity C

Table 11: LNCaP-ENR Percent Cell Viability at Various Daclatasvir Impurity C Concentrations

Percent Cell Viability		
6 µM	**8 µM**	**12 µM**
91.6500994	101.1928429	102.6838966
93.33996024	97.2166998	90.05964215
100.7952286	111.9284294	81.90854871

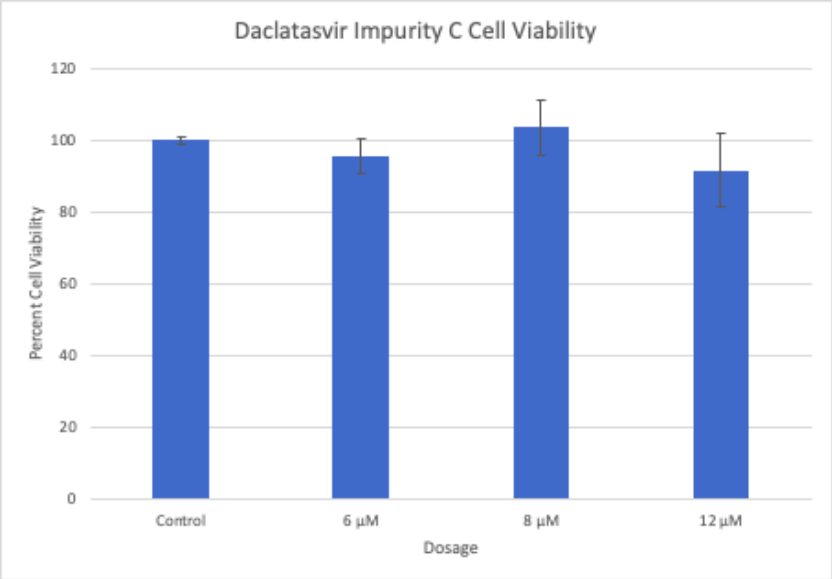

Figure 11: Bar Graph Indicating Mean Percent Cell Viability for LNCAP-ENR cells at different concentrations of Daclatasvir Impurity C

Velpatasvir 12

Table 12: LNCaP-ENR Percent Cell Viability at Various Velpatasvir 12 Concentrations

Percent Cell Viability			
4 µM	**8 µM**	**12 µM**	**16 µM**
97.01789264	96.22266402	96.81908549	93.73757455
101.0934394	100.3976143	95.62624254	96.22266402
100	89.26441352	98.31013917	99.70178926

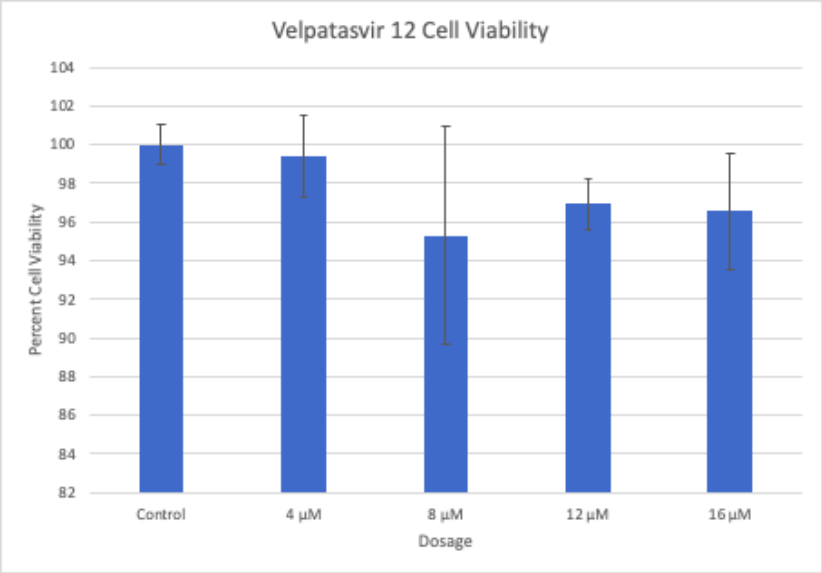

Figure 12: Bar Graph Indicating Mean Percent Cell Viability for LNCAP-ENR cells at different concentrations of Velpatasvir 12

Darapladib

Table 13: LNCaP-ENR Percent Cell Viability at Various Darapladib Concentrations

Percent Cell Viability			
1 µM	**2 µM**	**4 µM**	**8 µM**
92.31678487	109.6926714	32.26950355	2.364066194
98.34515366	112.4113475	23.40425532	2.127659574
99.52718676	101.4184397	34.86997636	2.718676123

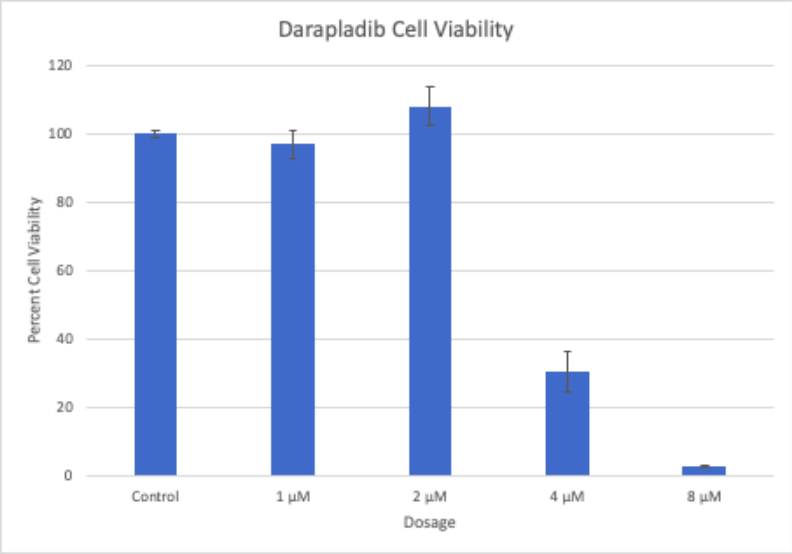

Figure 13: Bar Graph Indicating Mean Percent Cell Viability for LNCAP-ENR cells at different concentrations of Darapladib

Varespladib

Table 14: LNCaP-ENR Percent Cell Viability at Various Varespladib Concentrations

Percent Cell Viability			
4 µM	**8 µM**	**12 µM**	**16 µM**
121.3709677	128.4274194	122.1774194	112.2983871
131.8548387	145.1612903	122.983871	123.5887097
124.1935484	130.2419355	121.3709677	117.5403226

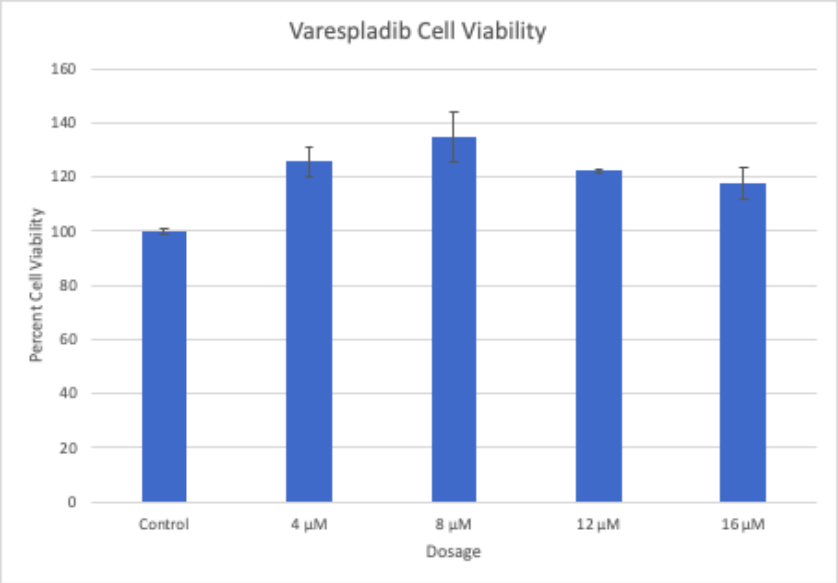

Figure 14: Bar Graph Indicating Mean Percent Cell Viability for LNCAP-ENR cells at different concentrations of Varespladib

AZD 4547

Table 15: LNCaP-ENR Percent Cell Viability at Various AZD 4547 Concentrations

Percent Cell Viability			
4 µM	**8 µM**	**12 µM**	**16 µM**
99.7983871	88.10483871	61.08870968	61.08870968
81.65322581	70.96774194	56.85483871	55.24193548
92.74193548	70.36290323	58.87096774	57.45967742

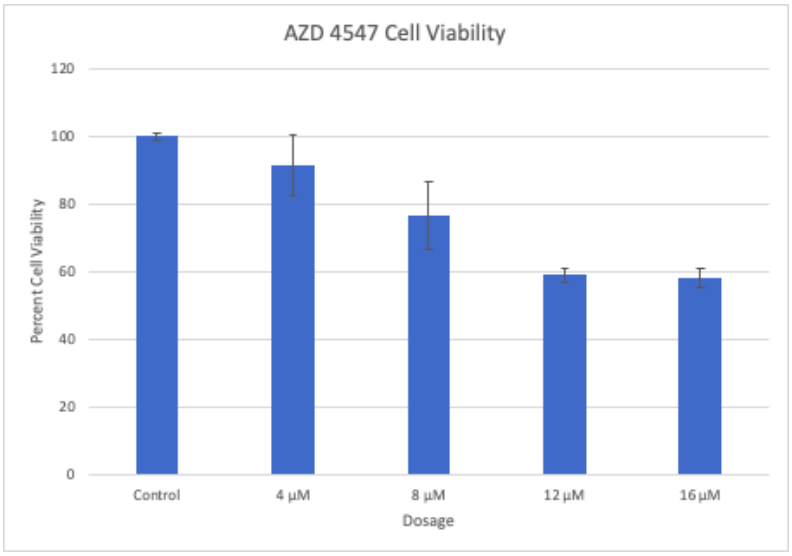

Figure 15: Bar Graph Indicating Mean Percent Cell Viability for LNCAP-ENR cells at different concentrations of AZD 4547

GW788388

Table 16: LNCaP-ENR Percent Cell Viability at Various GW788388 Concentrations

Percent Cell Viability			
4 µM	**8 µM**	**12 µM**	**16 µM**
128.8306452	116.9354839	101.4112903	101.6129032
109.6774194	106.25	95.36290323	91.33064516
99.7983871	103.4274194	102.8225806	105.6451613

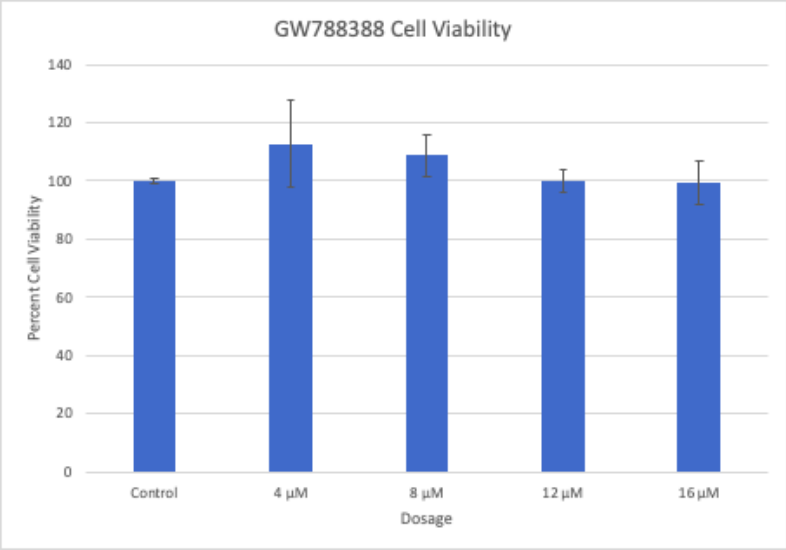

Figure 16: Bar Graph Indicating Mean Percent Cell Viability for LNCAP-ENR cells at different concentrations of GW788388

Cisplatin

Table 17: LNCaP-ENR Percent Cell Viability at Various Cisplatin Concentrations

Percent Cell Viability			
4 µM	**8 µM**	**12 µM**	**16 µM**
115.5241935	120.3629032	120.9677419	115.3225806
110.6854839	109.0725806	120.766129	134.4758065
113.7096774	83.06451613	114.516129	135.8870968

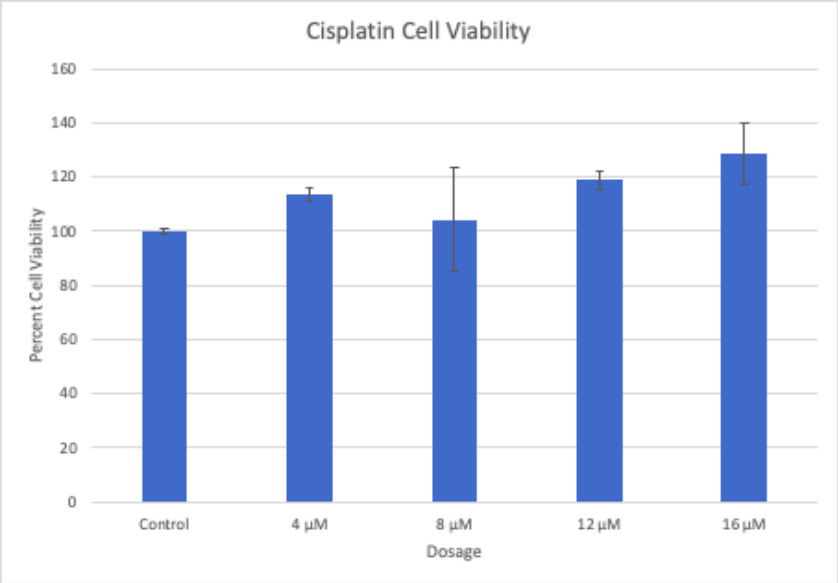

Figure 17: Bar Graph Indicating Mean Percent Cell Viability for LNCAP-ENR cells at different concentrations of Cisplatin

Navetiab

Table 18: LNCaP-ENR Percent Cell Viability at Various Navetiab Concentrations

Percent Cell Viability			
4 µM	**8 µM**	**12 µM**	**16 µM**
87.2983871	77.82258065	59.07258065	67.74193548
377.4193548	81.25	64.11290323	44.35483871
96.97580645	94.95967742	71.77419355	48.99193548

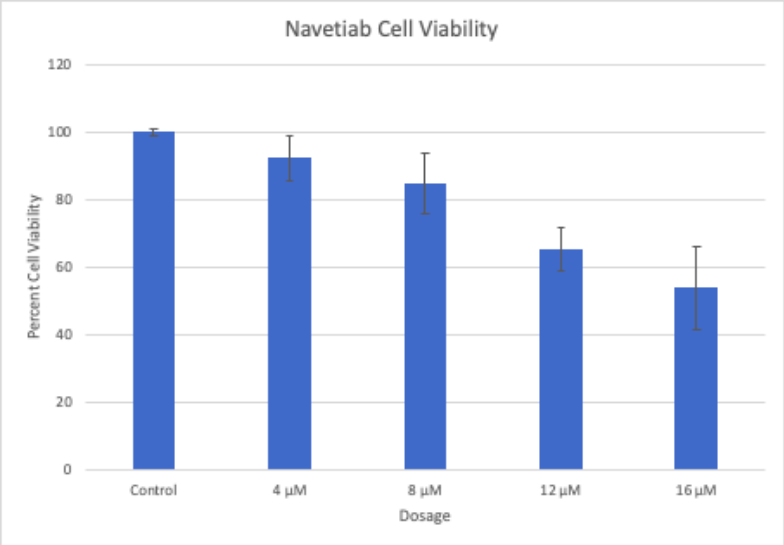

Figure 18: Bar Graph Indicating Mean Percent Cell Viability for LNCAP-ENR cells at different concentrations of Navetiab

Afatiab

Table 19: LNCaP-ENR Percent Cell Viability at Various Afatiab Concentrations

Percent Cell Viability			
4 µM	**8 µM**	**12 µM**	**16 µM**
111.4919355	64.11290323	57.66129032	53.02419355
95.36290323	73.79032258	72.58064516	51.20967742
85.48387097	59.47580645	57.45967742	54.63709677

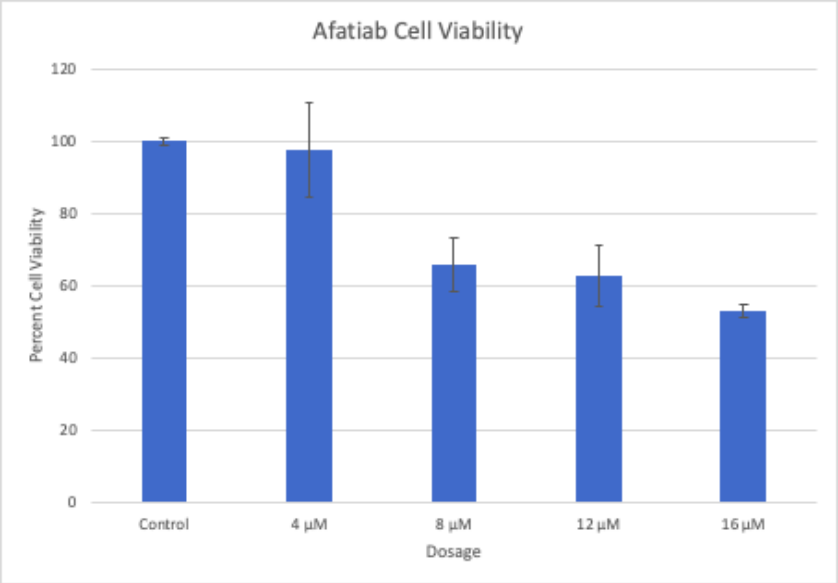

Figure 19: Bar Graph Indicating Mean Percent Cell Viability for LNCAP-ENR cells at different concentrations of Afatiab

Daclatasvir(Selleck)

Table 20: LNCaP-ENR Percent Cell Viability at Various Daclatasvir(Selleck) Concentrations

Percent Cell Viability				
4 µM	**8 µM**	**12 µM**	**16 µM**	**20 µM**
89.09657321	87.69470405	78.97196262	75.54517134	93.92523364
88.94080997	86.13707165	77.25856698	95.63862928	86.44859813
120.8722741	121.9626168	106.3862928	110.1246106	126.9470405

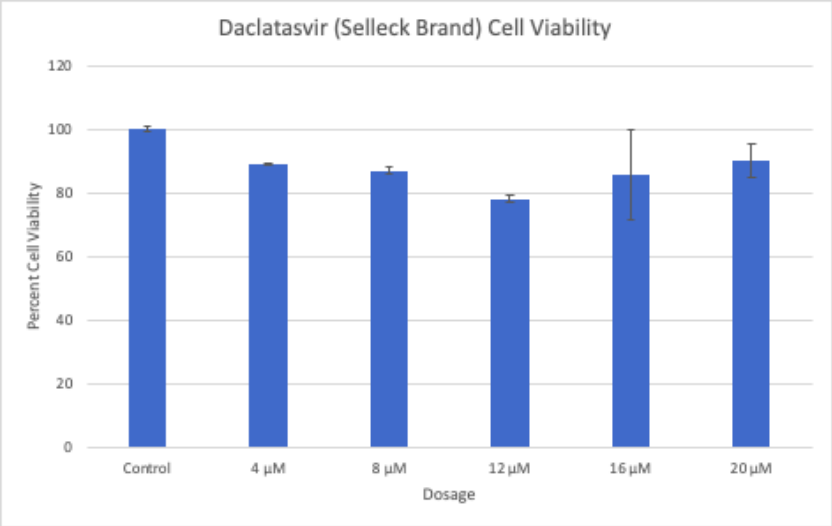

Figure 20: Bar Graph Indicating Mean Percent Cell Viability for LNCAP-ENR cells at different concentrations of Daclatasvir (Selleck Brand)

Verteporfin

Table 21: LNCaP-ENR Percent Cell Viability at Various Verteporfin Concentrations

Percent Cell Viability			
2 µM	**4 µM**	**8 µM**	**12 µM**
8.885298869	16.47819063	10.50080775	16.80129241
11.14701131	15.02423263	11.63166397	15.02423263
9.8546042	14.86268174	15.34733441	15.83198708

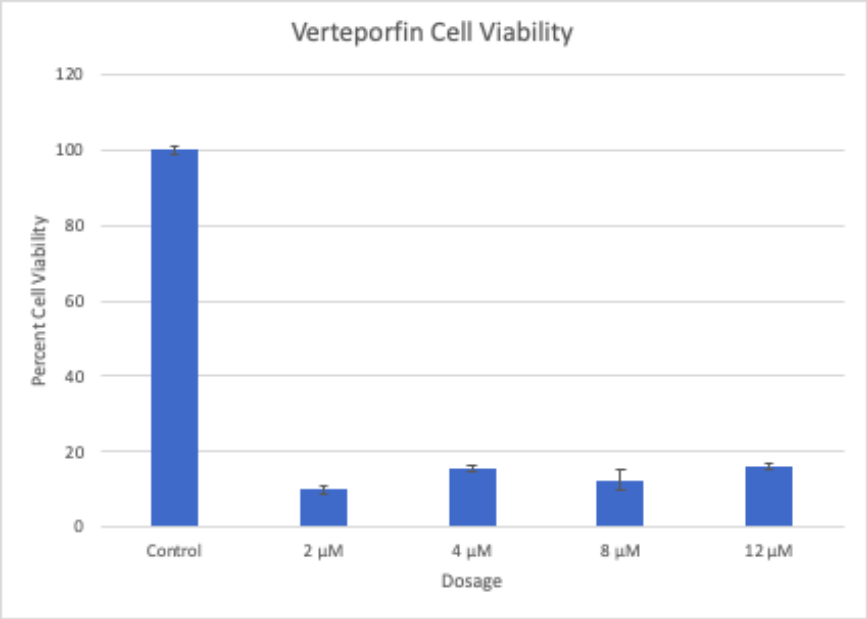

Figure 21: Bar Graph Indicating Mean Percent Cell Viability for LNCAP-ENR cells at different concentrations of Verteporfin

Ca3

Table 22: LNCaP-ENR Percent Cell Viability at Various Ca3 Concentrations

Percent Cell Viability			
2 µM	**4 µM**	**8 µM**	**12 µM**
39.09531502	32.79483037	30.21001616	28.43295638
33.60258481	34.89499192	36.18739903	26.97899838
40.54927302	31.82552504	30.53311793	24.71728595

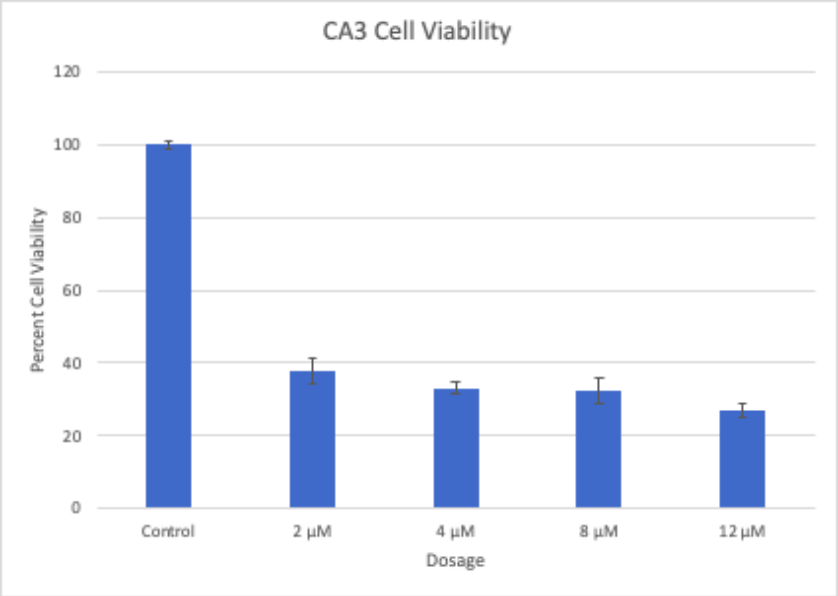

Figure 22: Bar Graph Indicating Mean Percent Cell Viability for LNCAP-ENR cells at different concentrations of CA3

JNK-Inhibitor 2

Table 23: LNCaP-ENR Percent Cell Viability at Various JNK-Inhibitor 2 Concentrations

Percent Cell Viability			
4 µM	**8 µM**	**12 µM**	**16 µM**
102.2016222	93.62688297	85.74739282	85.05214368
84.82039397	86.79026651	82.38702202	92.69988413
87.6013905	74.1599073	82.85052144	87.02201622

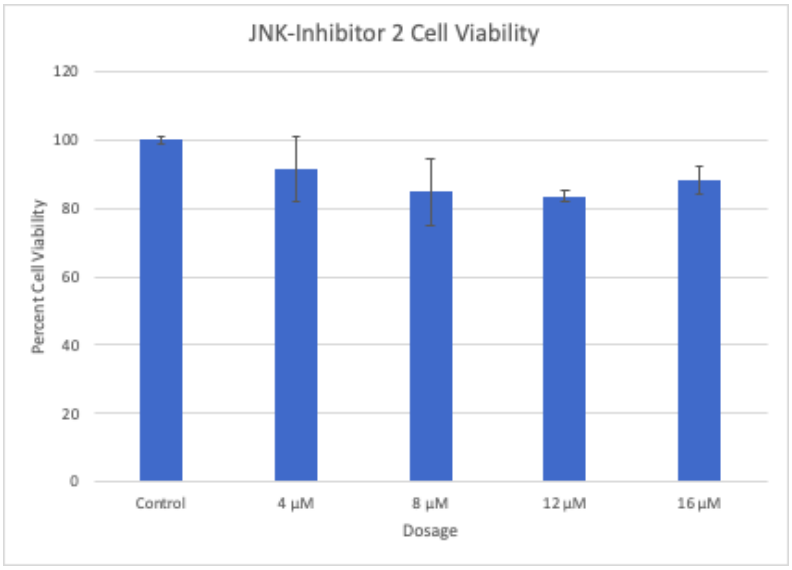

Figure 23: Bar Graph Indicating Mean Percent Cell Viability for LNCAP-ENR cells at different concentrations of JNK-Inhibitor 2

GSK 3β Inhibitor VIII

Table 24: LNCaP-ENR Percent Cell Viability at Various GSK 3β Concentrations

Percent Cell Viability			
4 µM	**8 µM**	**12 µM**	**16 µM**
86.67439166	84.2410197	67.4391657	68.71378911
94.55388181	83.42989571	77.75202781	61.18192352
78.67902665	72.19003476	62.45654693	62.10892236

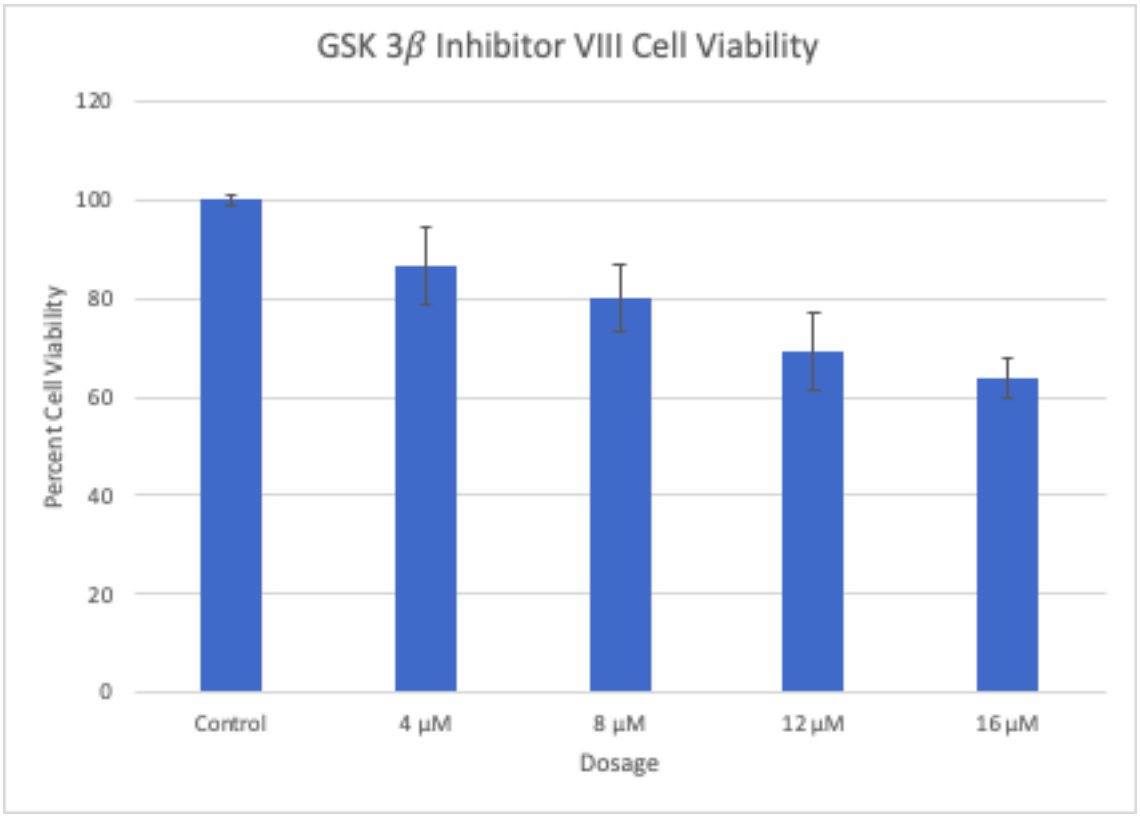

Figure 24: Bar Graph Indicating Mean Percent Cell Viability for LNCAP-ENR cells at different concentrations of GSK 3β Inhibitor

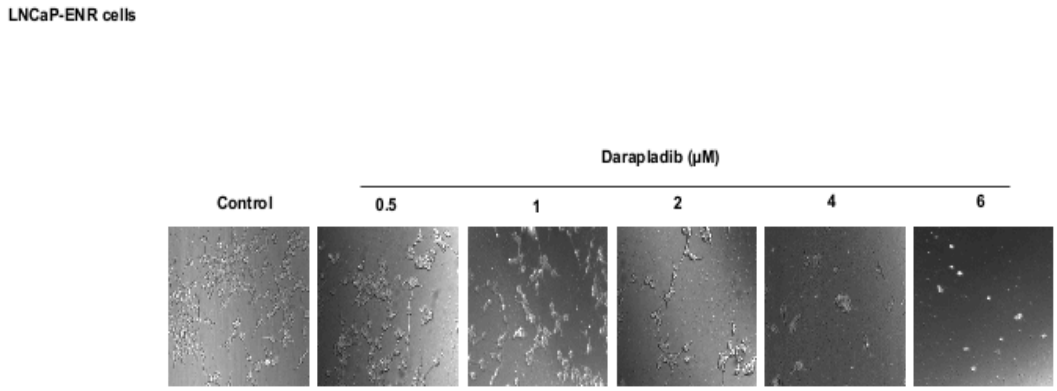

Figure 25: Cell Morphology of LNCaP-ENR cells treated at different concentrations of Darapladib

Discussion

In this research, we sought to identify compounds from a novel library which were effective in inducing apoptosis in advanced prostate cancer cells. Specifically, we observed the effect of these compounds on LNCaP cells that are resistant to enzalutamide, as it is one of the leading causes of death in patients dealing with prostate cancer. In order to differentiate effective and noneffective compounds, the percent cell viability at each dose of the compound was calculated. This calculation was done by comparing the absorbance values of the control wells with the experimental wells, while also controlling for the absorbance value given by wells solely containing media. An effective compound would show a decrease in percent cell viability as the dosage of the compound increased, while a non-effective compound would either have a percent cell viability close to a 100% or have an inconsistent trend in regards to percent cell viability as the dosage increased. Based on this criteria, we identified three effective compounds that had potential inhibitory effects on advanced prostate cancer cells. These compounds were AZD-9291, XMD8-92, and Darapladib. AZD-9291 shows a decrease in percent cell viability as dosage increases especially as the dosage increases from 4 μM to 8 μM which can be seen in figure 4. XMD8-92 showed a similar trend with a sharp decrease in percent cell viability from 2 μM to 4 μM. Although the percent cell viability was a bit higher than the control at 1μM, this could be explained by a pipetting error which added a slightly higher cell concentration to the experimental wells than the cell concentration in the control wells. Darapladib showed the most significant decrease in percent cell viability as cell death increased drastically from a dosage of 2 μM to 4 μM. Similar to the percent cell viability for XMD8-92 at 1 μM, the percent cell viability

exceeding a 100% at 2 μM for Darapladib could be due to pipetting errors which increased the cellular concentration in the cell.

An important issue to note is that, due to time limitations, the assays conducted using the three effective compounds identified were not replicated. Therefore, the data collected on these compounds have not been verified for reproducibility. Thus, for researchers looking to verify this data they may want to consider conducting at least three biological replicates for each of the compounds of interest.

From the three effective compounds that were identified, Darapladib exhibited the most inhibitory potential as it decreased the percent cell viability significantly with a relatively small dosage increase. To further display the apoptotic effect of Darapladib, LNCaP-ENR cells were plated in several mini plates at a population of approximately 200,000 cells. Each plate was treated with a different concentration of Darapladib ranging from 0 μM to 6 μM. These plates were much larger than the wells in the 96-well plate making it much easier to visualize the effects of Darapladib on the prostate cancer cells. The cell morphology of each plate is shown in figure 25 where it can be clearly seen that Darapladib significantly reduces the cellular population as the dosage increases.

Future Study

In the future, we would like to conduct studies that further examine the apoptotic mechanism by which Darapladib inhibits LNCaP-ENR cell proliferation. This can be achieved by identifying proteins released by the cell when Darapladib is treated through assays such as Western Blotting. Once these proteins are found, we can identify which apoptotic pathway/pathways are implemented using the information we know about different apoptotic

mechanisms. Eventually, Darapladib may be a useful compound in combating enzalutamide resistant advanced prostate cancer and increase quality of life for patients.

References

Advanced prostate cancer. (n.d.). Retrieved March 08, 2021, from https://www.urologyhealth.org/urology-a-z/a_/advanced-prostate-cancer

Beer, T. M., & Bubalo, J. S. (2001, August). Complications of chemotherapy for prostate cancer.
Retrieved March 09, 2021, from https://pubmed.ncbi.nlm.nih.gov/11561990/

Board, P. (2020, October 09). Prostate cancer treatment (pdq®). Retrieved March 09, 2021, from https://www.ncbi.nlm.nih.gov/books/NBK65915/#CDR0000062965__107

Cell-Titer Glo 2.0 Assay. (2018). Retrieved April 04, 2021, from https://www.promega.com/-/media/files/resources/protocols/technical-manuals/101/celltiterglo-2-0-assay-protocol.pdf?la=en

Descotes, J. (2019, April). Diagnosis of prostate cancer. Retrieved March 08, 2021, from https://www.ncbi.nlm.nih.gov/pmc/articles/PMC6488713/

ED;, K. (2011, November). Characterising the castration-resistant prostate cancer population: A systematic review. Retrieved March 08, 2021, from https://pubmed.ncbi.nlm.nih.gov/21995694/

Elmore, S. (2007, June). Apoptosis: A review of programmed cell death. Retrieved March 09, 2021, from https://www.ncbi.nlm.nih.gov/pmc/articles/PMC2117903/

Fadok, V. A., Cathelineau, A. D., Henson, P. M., Bratton, D. L., & Daleke, D. L. (2012, January 01). Loss of Phospholipid Asymmetry and Surface Exposure of Phosphatidylserine Is Required for Phagocytosis of Apoptotic Cells by Macrophages and FibroblastsValerie. Retrieved March 09, 2021, from https://www.jbc.org/article/S0021-9258 (18)44118-X/fulltext

Garcia-Gutierrez, L., Delgado, M. D., & Leon, J. (2019). MYC Oncogene Contributions to

Release of Cell Cycle Brakes. *Genes, 10* (244), 1-29.

Ghosh, J. (2004, February 04). Rapid induction of apoptosis in prostate cancer cells by selenium:Reversal by metabolites of arachidonate 5-lipoxygenase. Retrieved April 04, 2021, from https://www.sciencedirect.com/science/article/pii/S0006291X04001408?via%3Dihub

Hahn, D. L., & Roberts, R. G. (1993). PSA Screening for Asymptomatic Prostate Cancer: Truth in Advertising. *The Journal of Family Practice, 37* (5), 432-436.

Hoimes, C., & Kelly, W. (2010, March 01). Redefining hormone resistance in prostate cancer. Retrieved March 08, 2021, from https://www.ncbi.nlm.nih.gov/pmc/articles/PMC2883184

How does the prostate work? (2016, August 23). Retrieved March 08, 2021, from https://www.ncbi.nlm.nih.gov/books/NBK279291/

Igney, F., & Krammer, P. (2002, April). Death and anti-death: Tumour resistance to apoptosis. Retrieved March 09, 2021, from https://www.nature.com/articles/nrc776

Kvale, R., Moller, B., Wahlqvist, R., Fossa, S. D., Berner, A., Busch, C., . . . Halvorsen, O. J. (2009, June). Concordance between Gleason scores of needle biopsies and radical prostatectomy SPECIMENS: A population-based study. Retrieved March 09, 2021, from https://pubmed.ncbi.nlm.nih.gov/19154461/

Li, Y., Mongan, J., Behr, S. C., Sud, S., Coakley, F. V., Simko, J., & Westphalen, A. C. (2016, June 17). Beyond prostate adenocarcinoma: Expanding the differential diagnosis in Prostate PATHOLOGIC CONDITIONS. Retrieved March 08, 2021, from https://pubs.rsna.org/doi/full/10.1148/rg.2016150226#:~:text=Prostate%20Anatomy,-Anatomically%2C%20from%20centrally&text=Prostate%20adenocarcinoma%20most%20commonly%20arises,at%20the%20apex%20and%20base.

Lichtenstein, P., Holm, N. V., Verkasalo, P. K., Iliadou, A., Kapprio, J., Koskenevuo, M., . . . Hemminki, K. (2000, July 13). Environmental and HERITABLE factors in the causation of cancer - analyses of cohorts of twins from Sweden, Denmark, and Finland: NEJM. Retrieved March 09, 2021, from https://www.nejm.org/doi/full/10.1056/NEJM200007133430201

Localized prostate cancer: Low-risk prostate cancer: Active surveillance or treatment? (2020, March 12). Retrieved March 09, 2021, from https://www.ncbi.nlm.nih.gov/books/NBK487255/

Lonergan, P. E., & Tindall, D. J. (2011). Androgen receptor signaling in prostate cancer development and progression. Retrieved March 09, 2021, from https://www.ncbi.nlm.nih.gov/pmc/articles/PMC3162670/

Madan, R. A., Gulley, J. L., & Kantoff, P. W. (2013, January). Demystifying immunotherapy in prostate cancer: Understanding current and future treatment strategies. Retrieved March 09, 2021, from https://www.ncbi.nlm.nih.gov/pmc/articles/PMC3556901/

Mazaris, E., & Tsiotras, A. (2013, July 1). Molecular pathways in prostate cancer. Retrieved March 09, 2021, from https://www.ncbi.nlm.nih.gov/pmc/articles/PMC3830904/

Osterling, J. E., Jacobsen, S. J., & Cooner, W. H. (1995, April). The use Of AGE-SPECIFIC reference ranges for Serum prostate specific antigen in MEN 60 years old or older. Retrieved March 08, 2021, from https://pubmed.ncbi.nlm.nih.gov/7532725/

Ravenna, L., Principessa, L., Verdina, A., Salvatori, L., Russo, M., & Petrangeli, E. (2014, May 6). Distinct phenotypes of human prostate cancer cells associate with different adaptation to hypoxia and pro-inflammatory gene expression. Retrieved April 04, 2021, from https://www.ncbi.nlm.nih.gov/pmc/articles/PMC4011733/

Rawla, P. (2019, April). Epidemiology of prostate cancer. Retrieved March 08, 2021, from

https://www.ncbi.nlm.nih.gov/pmc/articles/PMC6497009/#:~:text=Although%20only%201%20in%20350,of%2065%20years%20%5B11%5D.

Reddien, P. W., Cameron, S., & Horvitz, H. R. (2001). Phagocytosis promotes programmed cell death in C. elegans. Retrieved March 09, 2021, from https://www.nature.com/articles/35084096

Routh, J. C. (2005, July 01). Adenocarcinoma of the Prostate: Epidemiological Trends, Screening, Diagnosis, and Surgical Management of Localized Disease. Retrieved 2021, from https://www.mayoclinicproceedings.org/article/S0025-6196 (11)61565-6/fulltext

Sun, H., Lesche, R., Li, D., Liliental, J., Zhang, H., Gao, J., . . . Wu, H. (1999, May 25). PTEN modulates cell cycle progression and cell survival by regulating phosphatidylinositol 3,4,5,-TRISPHOSPHATE and akt/protein Kinase B signaling pathway. Retrieved March 09, 2021, from https://www.ncbi.nlm.nih.gov/pmc/articles/PMC26859/

Ventola, C. (2017, August). Cancer immunotherapy, Part 3: Challenges and future trends. Retrieved March 09, 2021, from https://www.ncbi.nlm.nih.gov/pmc/articles/PMC5521300/#:~:text=These%20include%20the%20inability%20to,efficacy%3B%20and%20high%20treatment%20costs.